

RANDOM PROJECTION AND MULTISCALE WAVELET LEADER BASED ANOMALY DETECTION AND ADDRESS IDENTIFICATION IN INTERNET TRAFFIC

R. Fontugne^{1,2}, P. Abry³, K. Fukuda¹, P. Borgnat³, J. Mazel^{1,2}, H. Wendt⁴, D. Veitch⁵

¹ National Institute of Informatics, Tokyo, Japan, romain@nii.ac.jp

² Japanese French Laboratory for Informatics, Tokyo, Japan,

³ CNRS, Ecole Normale Supérieure de Lyon, France, patrice.abry@ens-lyon.fr

⁴ CNRS, ENSEEIHT-Toulouse, France, ⁵ Dept. EEE, University of Melbourne, Australia,

Supported by CNRS-JSPS France-Japan grant, ANR BLANC 2011 AMATIS BS0101102, Strategic International Collaborative R&D Promotion Program of the Ministry of Internal Affairs and Communication, Japan, and EU FP7/2007-2014, grant 608533 (NECOMA)

ABSTRACT

We present a new anomaly detector for data traffic, ‘SMS’, based on combining random projections (sketches) with multiscale analysis, which has low computational complexity. The sketches allow ‘normal’ traffic to be automatically and robustly extracted, and anomalies detected, without the need for training data. The multiscale analysis extracts statistical descriptors, using wavelet leader tools developed recently for multifractal analysis, without any need for timescales to be selected a priori. The proposed detector is illustrated using a large recent dataset of Internet backbone traffic from the MAWI archive, and compared against existing detectors.

Index Terms— Multifractal analysis, multiscale representation, random projection, anomaly detection, Internet traffic.

1. INTRODUCTION

Context: Internet traffic monitoring. Research into Internet traffic measurement has been extensive, ranging from data capture systems, through to statistical analysis, data modeling and prediction. The goals of this activity include insights to better design and operate the network, to optimize resources and performance, and to address security issues. The detection of anomalies is a crucial network monitoring task as it impacts at multiple levels including the diagnosis of network dysfunction, localization of performance bottlenecks, and discovery of unusual traffic including malicious activity.

Anomaly detection in computer network traffic context is highly challenging. First there is the variable nature of the data itself, which may be available at levels of granularity that differ in time (from μ s to daily averages), in geographic spread (single link/router or multiple, core or access networks), or in detailed nature (packet timestamps, sizes, 5-tuples¹, or application level data). Second, the origins of anomalies are diverse and include the physical layer, IP protocols, application layer protocols, source traffic events such as flashcrowds, and ‘heavy hitter’ or ‘ α -flows’. Anomalies due to malicious activity include those whose signature is well known, for example Distributed Denial of Service (DDoS) and port scanning, but new forms of attack, resulting in new anomalies which may be very subtle, regularly appear. This variety implies anomalous traffics whose forms and statistics show very different kinds of departures from normal

traffic, which precludes the use of *matched filter* approaches, even if adaptive and advanced. Third, *normal* traffic is itself an ill-defined notion, and the construction of a traffic reference, against which anomalies can be defined, is non-trivial, in particular since traffic characteristics naturally vary over time with the evolution of applications and services. This significantly impairs the use of supervised classification strategies, as training sets of expert-annotated anomalies will in general be unavailable. Fourth, the very high volume of Internet traffic restricts the complexity of statistical features that can be routinely computed. Finally, privacy concerns may also constitute a barrier to anomaly detection.

Related works: anomaly detection. We focus on anomaly detection based on aggregated time series, being counts of IP packets or bytes in consecutive time bins, obtainable from packet header traces containing timestamps plus 5-tuples for each packet. This approach has the advantage of being more privacy-friendly than techniques that rely on packet payload, and remains relevant in the face of payload encryption techniques such as IPsec. Another advantage of time series is that existing signal statistical processing detection/classification tools are available, including many with low computational cost, suitable for long time series.

Among unsupervised approaches applied to univariate time series, wavelet filtering has been used to select relevant time scales for detection [1]. Entropy-based detectors applied to specific features (IP addresses and port numbers [2, 3, 4], connection patterns [5]) have also proved successful. Exploiting the scale invariance properties of Internet traffic [6, 7], anomaly detection has also been based on the self-similarity parameter [8, 9]. For multivariate data (multi-link/point measurements), Principal Component Analysis (PCA) allows a reference traffic to be computed, and thus to quantify anomalous deviations from it [10]. In an attempt to capture different classes of anomalies, multimodal detection procedures were also attempted. For example, *Astute* [11] monitors packet and byte counts jointly at six different aggregation levels. Random projection tools, also known as *hashing* procedures or *sketching*, were also used for the automatic construction of reference traffic [12, 13]. To do this they exploited the flow-level structure of IP traffic. Other works which exploit flow structure include [3, 4, 8].

Goals, contributions and outline. This paper proposes a network traffic anomaly detection procedure, called *Sketch and MultiScale* (SMS), based on the analysis of packet count time series assembled from 5-tuple plus timestamp data. The procedure is unsupervised, and is therefore suitable for the detection of new anomaly types as

¹The standard 5-tuple consists of five IP packet header fields: IP address and port number for source and destination, and IP protocol carried (TCP, UDP or ICMP). Timestamps may be combined with 5-tuples to define *flows*.

well as old, and avoids the need for training sets. Instead, it uses multiple flow-preserving sketches to extract a reference ‘normal’ traffic from the trace itself. Each sketch yields a time series which is analysed using wavelet-leader based multiscale representations, recently designed for the most up-to-date formalism for practical multifractal analysis [14]. These result in fast, robust, multiscale representations of the statistical properties of the time series, defined over a set of time scales ranging from milliseconds to minutes (over 5 decades). This avoids the a priori selection of time scales at which anomalies should be seen and make it feasible to process very large traces. Finally, comparing across independent sets of sketches allows the flow-defining IP addresses involved in the anomaly to be isolated.

Random projections and wavelet leaders are presented in Section 2.1 and 2.2 respectively, while the anomaly detection and anomalous flow identification is detailed in Section 2.3. We put SMS to work on a large recent Internet dataset (1st half of 2014), part of the Japanese MAWI repository [15], described in Section 3. Detection performance is quantified and interpreted qualitatively in Section 4, and compared against that obtained with MAWILab [16], the reference tool of the MAWI repository.

2. METHODOLOGY

For each packet i in a given trace, arriving at time t_i , we assign a flow label A_i based on its 5-tuple. Here we use $A_i \in \{\text{IPsrc}_i, \text{IPdst}_i\}$.

2.1. Random projections / Sketches

A random projection of an IP trace X consists of a hash function, acting on flow labels, which inserts the packets of X into a hashtable of size M , resulting in a random flow-splitting of X into M sub-traces X_m , $m \in \{1, \dots, M\}$. In other words, all packets of any given flow are allocated together to a randomly chosen entry in the hashtable. If there are no anomalies, then we expect each sub-trace, or *sketch*, to be statistically equivalent (and moreover equivalent to the full trace up to a constant variance factor assuming independence between flows). The intuition here is that anomalies in X will only be present in some of its sketches. A median over sketches can therefore provide a reference for normal traffic that shows little sensitivity to the outlier sketches carrying the anomalies. Furthermore, anomalies will be easier to detect in sketches where they appear, as the volume of normal traffic is reduced (higher signal to noise ratio).

A random projection procedure [12, 13] consists of $\{h_n, n = 1, \dots, N\}$ k -universal hash functions [17], giving rise to N independent sets of M sketches, and NM packet count timeseries $X_{n,m}$.

2.2. Wavelet-leader multiscale representations

It is well-accepted that Internet traffic statistics are well-characterized by scale invariance properties, notably self-similarity and long-memory [6], and that such scaling can be efficiently analyzed using multiscale representations, in particular based on wavelet decompositions [7]. It has also been proposed that scaling in Internet traffic can be modeled by multifractal models [18, 19], and that multifractal properties are best analyzed using *wavelet leader* based representations [14]. Wavelet-leader based multiscale representations are therefore a natural choice as a basis for anomaly detection.

Wavelet coefficients. Let ψ denote the mother wavelet, characterized by a strictly positive integer N_ψ , defined as $\int_{\mathbb{R}} t^k \psi(t) dt \equiv 0 \forall n = 0, \dots, N_\psi - 1$, and $\int_{\mathbb{R}} t^{N_\psi} \psi(t) dt \neq 0$, known as the number of vanishing moments. The (L^1 -normalized) discrete wavelet transform coefficients $d_X(j, k)$ of the process X are defined as

$d_X(j, k) = \langle \psi_{j,k} | X \rangle$, with $\{\psi_{j,k}(t) = 2^{-j} \psi(2^{-j}t - k)\}_{(j,k) \in \mathcal{N}^2}$. For a detailed introduction to wavelet transforms see [20].

Wavelet leaders. Let $\lambda_{j,k} = [k2^j, (k+1)2^j)$ denote the dyadic interval of size 2^j centered at $k2^j$, and $3\lambda_{j,k}$ the union of $\lambda_{j,k}$ with its left and right neighbors: $3\lambda_{j,k} = \bigcup_{m \in \{-1, 0, 1\}} \lambda_{j, k+m}$. The *wavelet leader* $L_X^{(\gamma)}(j, k)$ is defined as the largest wavelet coefficient in the neighborhood $3\lambda_{j,k}$ over all finer scales $j' < j$ [14]:

$$L_X^{(\gamma)}(j, k) := \sup_{\lambda' \subset 3\lambda_{j,k}} |2^{j'\gamma} d_X(\lambda')|. \quad (1)$$

The parameter $\gamma \geq 0$ must be chosen to ensure a minimal regularity constraint (see [14] for a theoretical study).

Log-cumulants. It has been shown the cumulants of order p , $C_p^\gamma(j)$, of $\ln L_X^{(\gamma)}(j, k)$ provide relevant representations of the statistics of X as a function of scale 2^j ([21, 14]). Notably, when X is characterized by multifractal properties, the $C_p^\gamma(j)$ take the explicit form

$$C_p^\gamma(j) = c_p^{0,(\gamma)} + c_p^{(\gamma)} \ln 2^j \quad (2)$$

where the $c_p^{(\gamma)}$ can be directly related to the *multifractal spectrum* of X (see [14, 22] for details). The attributes $c_p^{(\gamma)}$ are not explicitly used here, instead SMS relies on the underlying multiscale representations $C_p^{(\gamma)}(j)$, where $C_1^{(\gamma)}(j)$ is mainly associated to the 2nd-order statistics of X (covariance or spectrum), while $C_2^{(\gamma)}(j)$ conveys information beyond 2nd-order statistics.

2.3. Sketch and MultiScale (SMS)

The anomaly detection and address identification procedure of SMS can be outlined as follows.

Step 1 For each trace, use the N hash functions to produce N sets of M sub-traces, and aggregate each one at resolution Δ_0 to produce the flow-sampled time series $X_{n,m}(t)$.

Step 2 For each $X_{n,m}$, compute wavelet-leader based $C_{p,n,m}^{(\gamma)}(j)$, $p = 1, 2$. For each n compute the median over the n -th set of M cumulants as $\overline{C}_{p,n}^{(\gamma)}(j) = \text{Median}\{C_{p,n,m}^{(\gamma)}(j), m = 1, \dots, M\}$.

Step 3 For each n and p , $\overline{C}_{p,n}^{(\gamma)}(j)$ constitutes a robust reference regarded as characteristic of normal traffic. The Euclidean distance of each sketch to its respective reference in set n is calculated as

$$\mathcal{D}_{p,n}^m = \frac{1}{1 + j_2 - j_1} \left(\sum_{j=j_1}^{j_2} (C_{p,n}^{(\gamma)}(j) - \overline{C}_{p,n}^{(\gamma)}(j))^2 \right)^{1/2}. \quad (3)$$

A sketch k in set n is reported, by cumulant p , as *suspicious* when its distance to its reference is large compared to the reference variation:

$$\mathcal{D}_{p,n}^k > \text{median}_m \{\mathcal{D}_{p,n}^m\} + \tau \text{MAD}_m \{\mathcal{D}_{p,n}^m\}, \quad (4)$$

where $\text{MAD} = \text{Maximum Absolute Deviation}$, and τ is a parameter.

Step 4 Let \mathcal{A}_n denote the set of all flow labels from suspicious sketches from the n -th table. This set contains many normal flows which will vary randomly from table to table, whereas anomalous flows will be found in multiple \mathcal{A}_n . We define a flow to be *suspicious* if it appears in at least ℓ of the \mathcal{A}_n .

3. MAWI TRAFFIC ARCHIVE

MAWI Repository. We evaluate SMS using Internet backbone traffic from the MAWI archive [15, 23], specifically from the

samplepoint-F transit link connecting several Japanese research institutes and universities to the Internet. Here packet header traces, collected daily from 14:00 to 14:15 (Japanese Standard Time), are anonymized and made publicly available. We use traces captured from the first 15 days of each of the first 6 months of 2014, a total of 78 excluding incomplete traces. Each trace contains roughly 100 to 150 million IP packets, corresponding to an average packet inter-arrival time (IAT) of the order of $7\mu\text{s}$.

MAWILab. MAWI traffic is currently monitored by MAWILab [16], a combination of four conventional detectors [8, 4, 24, 25], based respectively on multiscale gamma distributions, entropies, Hough transforms and association rules, that incorporates automated reporting and documentation of anomalies.

4. RESULTS

Parameter settings. For random projections, we set $N = 8$, $M = 16$, and adopt the h_n from [17]. The aggregation time (bin size) is set to $\Delta_0 = 2^{-3} = 0.125\text{ms}$, close to the sketch average IAT of $0.115\text{ms} \approx 16 \times 7\mu\text{s}$. Cumulants of order $p = 1, 2$ with $\gamma = 1$ (thus,

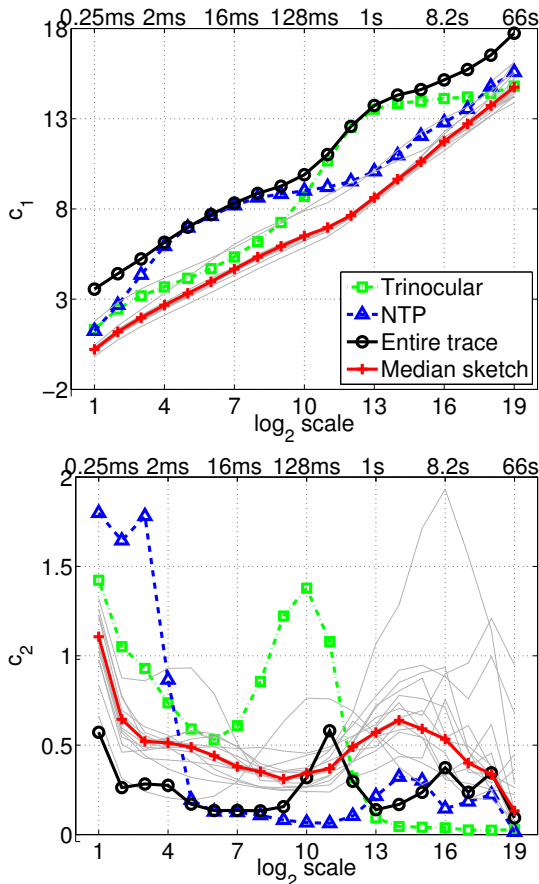


Fig. 1. Analysis Example: MAWI trace 2014/01/05. $C_1(j)$ (top) and $C_2(j)$ (bottom) computed for the entire trace (solid black line with ‘o’), each of the M sketches (light gray) and median $\bar{C}_p(j)$ (solid red with ‘+’). The median (normal) $C_1(j)$ is free of prominent anomalies and exhibits biscaling. Two sketches contain prominent anomalies: trinocular (green dash-dot line) and NTP (blue dashed).

mean and variance of $\ln L_X^{(\gamma)}(j, k)$) are used as suggested for Internet traffic statistical characterization in [22]. The detection threshold for suspicious sketches is set to $\tau = 3$. This value was found empirically to control false positives, and allows (4) to be viewed as a robust form of ‘ $\mu + 3\sigma$ ’. The detection threshold for suspicious flows is set to $\ell = 7$, since $\ell = 8$ frequently yielded no candidates (N too small given the sensitivity of the underlying detector for this data), and the false positive rate is monotonically decreasing in ℓ .

Introduction. We begin with an example of the analysis procedure over a representative trace, using a single hashtable with IPsrc as flow key. The top plot of Fig. 1 reports $C_1(j)$ computed for each sketch. All but two almost superimpose (grey lines), and these define the sketch-median $\bar{C}_1(j)$, whereas the two outliers are detected as suspicious. The same holds in the bottom plot for $C_2(j)$.

Although only two sketches are suspicious, the $C_p(j)$ computed from the entire trace is mostly dominated by them, showing the danger of performing statistical analysis blindly on full traces. Inconsistent and difficult to interpret results will be obtained, as the nature of anomalies varies from day to day. Instead, the proposed procedure allows the robust extraction of normal traffic and the characterization of its statistical properties, and thereby the unveiling of anomalies.

Fig. 1 shows that the median sketch $\bar{C}_1(j)$ (red) exhibits *biscaling*: two different scale ranges separated by a ‘knee’, here at $j = 12$ (0.5s). Originally reported in [26], this is now commonly considered as a signature of normal traffic. To avoid a failure of statistical robustness at small (too close to the IAT) or large (limit of trace duration) scales, we restrict analysis to $\mathbf{J} = (j_1, j_2) = (4, 16)$ (2ms to 8s). For $C_2(j)$, it is now documented [22] that a relevant range, where multifractality is shown, is $(j_1, j_2) = (2, 10)$ (0.5-128ms).

Let $\bar{D}_{p,n}^m = |\mathcal{D}_{p,n}^m - \text{median}(\mathcal{D}_{p,n}^m)| / \text{MAD}(\mathcal{D}_{p,n}^m)$ denote the normalized sketch distance. Fig. 2 provides an overview of all the sketch summaries by superimposing the NM normalized distance pairs $(\bar{D}_{1,n}^m, \bar{D}_{2,n}^m)$ for each of the 78 traces, using IPsrc (left) or IPdst (right) flow keys. The thresholds defining suspicious sketches appear at $\tau = 3$ (dashed red lines). The percentages shown give the proportions of these detected by C_1 or C_2 alone, or both.

Two Important Anomaly Classes. A manual inspection of the suspicious flows extracted from the suspicious sketches from Fig. 1 confirmed them to be anomalies belonging to two particular classes.

The first consists of reflection DDoS attacks based on the Network Time Protocol (NTP) [27]. Here NTP query traffic sent by the attacker is amplified by triggering NTP servers to ‘reflect’ a large message to the victim. Like most protocols susceptible to reflection attacks, the NTP protocol is carried by UDP, a connectionless protocol that allows the reflected traffic to be sent in a tight burst. Consequently, the compromised server sends packets at an abnormally high rate, visible in both $C_1(j)$ and $C_2(j)$ at fine time scales

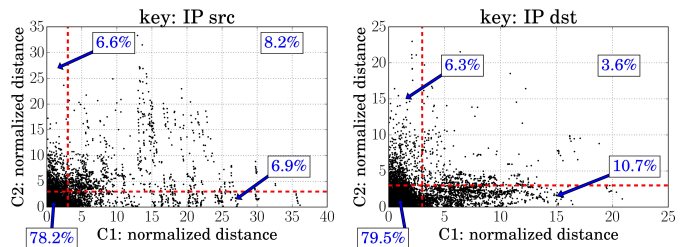


Fig. 2. Normalized sketch distance pairs over all traces. The dashed lines mark the thresholds defining suspicious sketches.

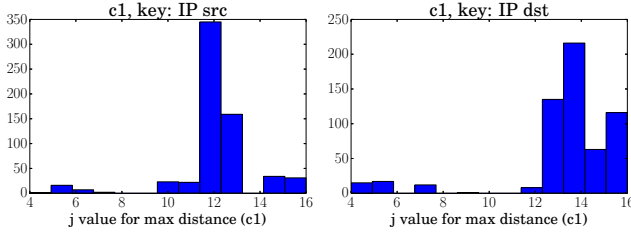


Fig. 3. Location j^* of C_1 -spikes (spike threshold = 0.1).

($j < 10$, or below 128ms), implying it impacts on both temporal correlations and higher order dependencies. Recent NTP reflection attacks have had a significant impact worldwide [27, 28].

The second class corresponds to the scanning activities of the *Trinocular* project [29]. Trinocular probes millions of computers on an ongoing basis in order to monitor their network connectivity, and to detect Internet outages. Because probes are all sent with a timeout of 3 seconds, the corresponding traffic shows a clear characteristic time scale, visible in $C_1(j)$ at coarse time scales ($j > 10$) and in $C_2(j)$ at $j = 10$ (roughly 128ms). This unusual though benign traffic has a similar appearance to malicious scans.

Anomaly Classification. Due to the huge volume of traffic data it is not feasible in general, nor here (almost 20,000 sketches were collected) to manually inspect all suspicious sketches and flows in order to provide the ground truth needed to assess detection performance using classical tools such as ROC curves. It is however indispensable to provide a practical means, beyond the conservative settings of thresholds detailed above, to ensure that detected anomalies are meaningful. To this end we make use of a recently proposed backbone traffic taxonomy [30] to classify suspicious flows into one of six categories, those heading the columns in Tables 1 and 2. This approach contributes to two objectives: (i) an estimated breakdown of anomaly causes, (ii) a check for false positives - the taxonomy is a set of independent context-aware checks which in principle should identify false positives by classifying them as ‘Other’.

To better understand the kinds of anomalies detectable by SMS, two types of suspicious sketches under C_1 are distinguished:

i) C_1 -shifts: those distant from the median \bar{C}_1 across all of \mathbf{J} . These are consistent with a volume change of a subset of traffic with the same characteristics as normal traffic;

ii) C_1 -spikes: those that are close to \bar{C}_1 except at some time scale $j^* \in \mathbf{J}$. These indicate traffic with anomalous characteristics.

Fig. 3 shows that the distribution of j^* for C_1 -spike sketches concentrates in the range 500 to 1000 ms. Thus, being close to the knee of biscaling, spikes strongly influence multiscale behaviour.

Applying SMS yielded 554 suspicious flows over all traces and both IPsrc and IPdst flows, broken down in Table 1 according to the taxonomy and five disjoint detection scenarios. The proportion classified as ‘Other’ is only $26/554 \approx 4.7\%$, an indication that the

	Scan	DoS	NTP	Pt.Multi.Pt.	α -Flow	Other	Total
C_1 -shift & C_2	37	2	2	40	9	1	91
C_1 -spike & C_2	23	1	9	4	1	0	38
C_1 -shift only	37	1	14	106	40	15	213
C_1 -spike only	70	0	3	6	0	5	84
C_2 -only	14	7	7	45	50	5	128
Total	181	11	35	201	100	26	554

Table 1. Detection detail of suspicious flows, and classification.

	Scan	DoS	NTP	Pt.M.Pt.	α -Flow	Other	Total
SMS	181	11	35	201	100	26	554
MAWILab	3626	94	105	2878	1178	260	8141
SMS \ MAWILab	44	11	26	81	93	12	267
MAWILab \ SMS	3489	94	96	2758	1171	246	7854
SMS \cap MAWILab	137	0	9	120	7	14	287
SMS \cup MAWILab	3670	105	131	2959	1271	272	8408

Table 2. Detection breakdown comparison: SMS and MAWILab.

false positive rate is low. The four volume based anomalies [Denial-of-Service (DoS), NTP reflection attacks (NTP), point-to-multipoint traffic (Pt.Multi.Pt.), and α -flows (α -Flow)] are mainly captured as C_1 shift and C_2 anomalies, corresponding to both a traffic volume change and subtle temporal changes beyond correlation. It is worth noting that C_2 -only detections, which includes 7/11 DoS and 50/100 α -Flow anomalies, imply that volume-based or correlation based procedures would fail to detect them. Manual inspection of the 7 DoS cases showed that 5 of them occurred on the same day, and consisted of many IP sources each sending 45 or fewer TCP SYN packets to the same network.

Anomalies detected as C_1 -spikes are mostly classified as Scan which implies ICMP or UDP traffic. Scanning injects packets with a typical rate, and hence time scale, which interferes with the entire dependence structure (correlation, C_1 , and beyond, C_2) of traffic.

Detector Comparison. Table 2 details the detections, classified according to the taxonomy, made by SMS and MAWILab over all traces and flow labels. Unsurprisingly, MAWILab detects many more anomalies than SMS, as it combines four different detectors, and multiple parameter settings for each. The main point here is that SMS provides a complementary detection ability: out of its 554 detections, 267 are new. Adding SMS to MAWILab would allow 12% (11/94) more DoS detections and 25% (26/105) more NTP ones.

The scan, point-to-multipoint and α -flow anomalies identified by SMS only (see ‘SMS \ MAWILab’ in Table 2) have similar characteristics to those detected by MAWILab, but they involve far fewer packets. This indicates a greater sensitivity of SMS in those cases. Moreover, out of the 26 NTP amplification attacks caught by SMS only, 13 are significant as they have very high bandwidth. These were captured using IPdst based flows, whereas MAWILab missed them because these attacks had few packets per individual (IPsrc,IPdst) pair.

5. CONCLUSIONS

We have proposed a multiscale, sketch and flow based detection procedure, *Sketch and MultiScale* (SMS), which has low computational cost, does not require sensitive payload data, has an ability to generate its own reference traffic automatically and robustly, and in many cases an ability to identify the flows causing the anomalies.

Although it is not feasible, due to a lack of authoritative ground truth, to assess the performance of SMS formally, the majority of the flows detected as suspicious were manually inspected and confirmed as anomalies. By using the anomaly taxonomy of [30], we were able not only to explain the classification of SMS’s detections in terms of the capabilities of the underlying multiscale representations $C_1^{(\gamma)}(j)$, and $C_2^{(\gamma)}(j)$, we argued that the taxonomy acts as a practical cross-check on the false positive rate, which was inferred to be low.

We found that SMS provides a useful complementary detection capability compared to the MAWILab detector-set, capable of finding both subtle and significant anomalies missed by the latter.

6. REFERENCES

- [1] P. Barford, J. Kline, D. Plonka, and A. Ron, "A Signal Analysis of Network Traffic Anomalies," *ACM SIGCOMM IMW '02*, pp. 71–82, 2002.
- [2] A. Lakhina, M. Crovella, and C. Diot, "Mining Anomalies Using Traffic Feature Distributions," *ACM SIGCOMM '05*, pp. 217–228, 2005.
- [3] X. Li, F. Bian, M. Crovella, C. Diot, R. Govindan, G. Iannaccone, and A. Lakhina, "Detection and Identification of Network Anomalies Using Sketch Subspaces," *ACM IMC '06*, pp. 147–152, 2006.
- [4] Y. Kanda, R. Fontugne, K. Fukuda, and T. Sugawara, "ADMIRE: Anomaly Detection Method Using Entropy-based PCA with Three-step Sketches," *Comput. Commun.*, vol. 36, no. 5, pp. 575–588, Mar. 2013.
- [5] G. Nychis, V. Sekar, D. G. Andersen, H. Kim, and H. Zhang, "An Empirical Evaluation of Entropy-based Traffic Anomaly Detection," *ACM IMC '08*, pp. 151–156, 2008.
- [6] W. E. Leland, M. S. Taqqu, W. Willinger, and D. V. Wilson, "On the Self-Similar Nature of Ethernet Traffic (Extended Version)," *Networking, IEEE/ACM Transactions on*, vol. 2, no. 1, pp. 1–15, 1994.
- [7] P. Abry, R. Baraniuk, P. Flandrin, R. Riedi, and D. Veitch, "Multiscale Nature of Network Traffic," *IEEE Signal Proc. Mag.*, vol. 19, no. 3, pp. 28–46, 2002.
- [8] G. Dewaele, K. Fukuda, P. Borgnat, P. Abry, and K. Cho, "Extracting Hidden Anomalies using Sketch and Non Gaussian Multiresolution Statistical Detection Procedures," *ACM SIGCOMM LSAD '07*, pp. 145–152, 2007.
- [9] A. Scherrer, N. Larrieu, P. Owezarski, P. Borgnat, and P. Abry, "Non-Gaussian and Long Memory Statistical Characterizations for Internet Traffic with Anomalies," *Dependable and Secure Computing, IEEE Transactions on*, vol. 4, no. 1, pp. 56–70, Jan 2007.
- [10] A. Lakhina, M. Crovella, and C. Diot, "Diagnosing Network-Wide Traffic Anomalies," *ACM SIGCOMM '04*, pp. 219–230, 2004.
- [11] F. Silveira, C. Diot, N. Taft, and R. Govindan, "ASTUTE: Detecting a Different Class of Traffic Anomalies," *ACM SIGCOMM '10*, pp. 267–278, 2010.
- [12] S. Muthukrishnan, "Data Streams: Algorithms and Applications," in *ACM SIAM SODA '03*, Jan. 2003, p. 413.
- [13] B. Krishnamurthy, S. Sen, Y. Zhang, and Y. Chen, "Sketch-based Change Detection: Methods, Evaluation, and Applications," in *ACM IMC '03*, 2003, pp. 234–247.
- [14] H. Wendt, P. Abry, and S. Jaffard, "Bootstrap for Empirical Multifractal Analysis," *IEEE Signal Processing Mag.*, vol. 24, no. 4, pp. 38–48, 2007.
- [15] WIDE Project, MAWI Traffic Archive. [Online]. Available: <http://mawi.wide.ad.jp/mawi/>
- [16] R. Fontugne, P. Borgnat, P. Abry, and K. Fukuda, "MAW-ILab : Combining Diverse Anomaly Detectors for Automated Anomaly Labeling and Performance Benchmarking," *ACM CoNEXT '10*, 2010.
- [17] M. Thorup and Y. Zhang, "Tabulation Based 4-Universal Hashing with Applications to Second Moment Estimation," in *ACM SIAM SODA '04*, Jan. 2004, pp. 615–624.
- [18] R. H. Riedi, M. S. Crouse, V. J. Ribeiro, and R. G. Baraniuk, "A Multifractal Wavelet Model with Application to Network Traffic," *IEEE Transactions on Information Theory*, vol. 45, no. 3, pp. 992–1018, 1999.
- [19] N. Hohn, D. Veitch, and P. Abry, "Multifractality in TCP/IP Traffic: the Case Against," *Computer Network Journal*, vol. 48, pp. 293–313, 2005.
- [20] S. Mallat, *A Wavelet Tour of Signal Processing*. San Diego, CA: Academic Press, 1998.
- [21] B. Castaing, Y. Gagne, and M. Marchand, "Log-similarity for turbulent flows," *Physica D*, vol. 68, pp. 387–400, 1993.
- [22] S. Jaffard, P. Abry, and H. Wendt, "Irregularities and Scaling in Signal and Image Processing: Multifractal Analysis," in *Benoit Mandelbrot: A Life in Many Dimensions*. World scientific publishing, 2014.
- [23] K. Cho, K. Mitsuya, and A. Kato, "Traffic Data Repository at the WIDE Project," in *USENIX 2000 Annual Technical Conference: FREENIX Track*, 2000, pp. 263–270.
- [24] R. Fontugne and K. Fukuda, "A Hough-transform-based Anomaly Detector with an Adaptive Time Interval," *ACM SIGAPP Appl. Comput. Rev.*, vol. 11, no. 3, pp. 41–51, Aug. 2011.
- [25] D. Brauckhoff, X. Dimitropoulos, A. Wagner, and K. Salamatian, "Anomaly Extraction in Backbone Networks using Association Rules," *ACM IMC '09*, pp. 28–34, 2009.
- [26] N. Hohn, D. Veitch, and P. Abry, "Cluster Processes: A Natural Language for Network Traffic," *IEEE Transactions On Signal Processing*, vol. 51, pp. 2229–2244, 2003.
- [27] C. Rossow, "Amplification Hell: Revisiting Network Protocols for DDoS Abuse," in *Proceedings of the 2014 Network and Distributed System Security (NDSS) Symposium*, February 2014.
- [28] J. Czyz, M. Kallitsis, M. Gharaibeh, C. Papadopoulos, M. Bailey, and M. Karir, "Taming the 800 Pound Gorilla: The Rise and Decline of NTP DDoS Attacks," in *ACM IMC '14 (to appear)*, Vancouver, BC, Canada.
- [29] L. Quan, J. Heidemann, and Y. Pradkin, "Trinocular: Understanding Internet Reliability Through Adaptive Probing," *ACM SIGCOMM '13*, pp. 255–266, 2013.
- [30] J. Mazel, R. Fontugne, and K. Fukuda, "Taxonomy of Anomalies in Backbone Network Traffic," in *Proceedings of the fifth International Workshop on TRaffic Analysis and Characterization (TRAC '14)*, 2014, pp. 30–36.